Published OnlineFirst October 29, 2012; DOI: 10.1158/0008-5472.CAN-12-1881

A Tumorigenic MLL-Homeobox Network in Human Glioblastoma Stem Cells

Marco Gallo[1], Jenny Ho[1], Fiona J. Coutinho[1,4], Robert Vanner[1,4], Lilian Lee[1], Renee Head[1], Erick K. M. Ling[1,5], Ian D. Clarke[1], and Peter B. Dirks[1,2,3,4,5]

Abstract

Glioblastoma growth is driven by cancer cells that have stem cell properties, but molecular determinants of their tumorigenic behavior are poorly defined. In cancer, altered activity of the epigenetic modifiers Polycomb and Trithorax complexes may contribute to the neoplastic phenotype. Here, we provide the first mechanistic insights into the role of the Trithorax protein mixed lineage leukemia (MLL) in maintaining cancer stem cell characteristics in human glioblastoma. We found that MLL directly activates the Homeobox gene *HOXA10*. In turn, HOXA10 activates a downstream Homeobox network and other genes previously characterized for their role in tumorigenesis. The MLL–Homeobox axis we identified significantly contributes to the tumorigenic potential of glioblastoma stem cells. Our studies suggest a role for MLL in contributing to the epigenetic heterogeneity between tumor-initiating and non–tumor-initiating cells in glioblastoma. *Cancer Res; 73(1); 417–27. ©2012 AACR.*

Introduction

Epigenetic regulators play a pivotal role in the etiology of multiple malignancies. Altered epigenomic landscapes have been identified in cancer cells compared with normal tissue (1–4), and add a layer of intricacy to the study of diseases that also tend to be mutationally unstable (5). The contribution of epigenetic factors to cellular heterogeneity in tumors has been poorly addressed and few mechanistic insights have been resolved, especially in human gliomas (6–10). In particular, the role of epigenetic factors in subpopulations of cells that drive tumorigenesis has only been partially addressed, and studies of glioma have mostly focused on proteins belonging to the Polycomb group (11, 12). Elucidation of aberrant epigenetic mechanisms in the tumor-initiating subpopulations holds promise for the identification of novel and targetable pathways.

The Trithorax group (TrxG) homolog *mixed lineage leukemia* (MLL) is an important epigenetic regulator during development and its role is especially well defined in hematopoiesis (13–15). MLL is a histone methyltransferase that catalyzes the methylation of histone 3 at lysine 4 (H3K4; ref. 16), thereby inducing a complex series of epigenetic modifications that result in positive regulation of downstream genes that are involved in the complex interplay of self-renewal and differentiation (17–19). MLL is also a driver of leukemogenesis, in a process that involves aberrant regulation of Homeobox (HOX) transcription factors, especially *HOXA9* and *HOXA10* (20–27). Therefore, MLL contributes to both normal and malignant stem cell function.

Alvarez-Buylla and colleagues recently showed that *Mll* is expressed in neural stem cells in the mouse subventricular zone and that *Mll* is required for *Dlx2* expression and neurogenesis (28, 29). In GBM cell lines, *MLL* was found to be expressed in hypoxic conditions (7). However, although mutations in *MLL2* and *MLL3* have been identified in human medulloblastoma (30), a specific functional role for these Trithorax proteins and MLL in malignancies of the brain has not been established.

Glioblastoma (GBM) is the most common primary brain tumor, characterized by dismal prognosis (median survival, 15 months) even when aggressive therapies based on tumor resection and concomitant chemotherapy and radiotherapy are implemented (31). Previous studies identified a HOX signature in GBM bulk samples (32–34). Specifically, it was shown that high expression of *HOXA9* (32) or *HOXA10* (33) were predictive of poor patient survival. *HOXA10* expression was also previously detected in neurosphere cultures derived from GBM samples (33, 35). However, the mechanism controlling *HOXA10* expression and the molecular role of HOXA10 in either bulk or GBM stem cells have not been addressed. Given the negative association between *HOXA10* expression and patient survival, a more complete understanding of the pathways upstream and downstream of this transcription factor are required. Furthermore, nothing is currently known on the specific role of HOX genes in the GBM stem cell fraction.

In this report, we present data that highlight an important contribution of MLL in directly activating *HOXA10* in GBM

Authors' Affiliations: [1]Program in Developmental and Stem Cell Biology, Arthur and Sonia Labatt Brain Tumour Research Centre; [2]Division of Neurosurgery, The Hospital for Sick Children; Departments of [3]Surgery, [4]Molecular Genetics, and [5]Laboratory Medicine and Pathobiology, University of Toronto, Toronto, Canada

Note: Supplementary data for this article are available at Cancer Research Online (http://cancerres.aacrjournals.org/).

Corresponding Author: Peter B. Dirks, The Hospital for Sick Children, 1504 Hill wing, 555 University Ave., Toronto, Ontario M5G 1X8, Canada. Phone: 416-813-8529; Fax: 416-813-4975; E-mail: peter.dirks@sickkids.ca

doi: 10.1158/0008-5472.CAN-12-1881

Published OnlineFirst October 29, 2012; DOI: 10.1158/0008-5472.CAN-12-1881

stem cells. HOXA10 then activates other Homeobox transcription factors, which also contribute to a Homeobox transcriptional program in GBM. Our data represent the first mechanistic description of an MLL-dependent epigenetic program in populations of GBM cells with stem-like characteristics.

Materials and Methods

Cell culture and primary tumor cells

Glioblastoma neural stem (GNS) and human fetal neural stem (NS) cells were grown in culture as previously described (36, 37). Briefly, flasks or 10-cm cell culture dishes were coated with poly-L-ornithine and laminin (both from Sigma). Cells were grown as adherent monolayers in serum-free Neurocult NS-A Basal (Stemcell Technologies) media, supplemented with 2 mmol/L L-glutamine, N2 and B27 supplements, 75 μg/mL bovine serum albumin, 10 ng/mL recombinant human EGF (rhEGF), 10 ng/mL basic fibroblast growth factor (bFGF), and 2 μg/mL heparin. Cells were harvested by mild accutase (Sigma) treatment. All NS cell cultures expressed NS cell markers and responded to differentiation cues by expressing lineage markers (data not shown).

Primary cells from GBMs were acutely dissociated in artificial cerebrospinal fluid (38) by treatment with an enzyme cocktail at 37°C, as previously described (39, 40). Cells were sorted for the cell surface marker CD15 (41) in either Aria-SC or Aria-CFI cell sorters.

Mouse husbandry

All mouse procedures were approved by The Hospital for Sick Children's Animal Care Committee. For orthotopic transplantations, mice were anesthetized with ketamine/xylazine. Thereafter, 200,000 GliNS1 cells were suspended in PBS and injected in the forebrain of nonobese diabetic/severe combined immunodeficient (NOD/SCID) mice with a G27 needle. The coordinates for the injection were 1 mm anterior of the bregma, 2 mm to the right of the midline, and 3 mm deep. Mouse brain fixation and histopathology were done as previously described (40).

Western blots and immunohistochemistry

Western blots were carried out with the following antibodies: anti-HOXA10 (1:1,000; sc-17159; Santa Cruz Biotechnology); anti-Actβ (1:5,000; A5441; Sigma-Aldrich); anti-MLL^C (1:1,000; 05-765; Millipore). Secondary antibodies: anti-goat::HRP (1:5,000; 805-035-180; Jackson ImmunoResearch Lab); anti-mouse::HRP (1:10,000–20,000; A9044; Sigma-Aldrich).

Immunohistochemical analysis was conducted on frozen or paraffin-embedded primary tumor sections. Antibodies used: rabbit anti-SOX2 (1:500; ab97959; Abcam); mouse anti-MLL^C (1:500 and 1:1,000). Secondary antibodies used: anti-rabbit::A568 (1:500; A11036; Invitrogen/Molecular Probes); anti-mouse::A488 (1:1,000; A11029; Invitrogen/Molecular Probes). Images were acquired using a Quorum WaveFX spinning disk confocal system (Zeiss Axiovert 200M; Quorum Technologies Inc.).

Quantitative real-time PCR, MLL chromatin immunoprecipitation, DNA quantitative PCR, and statistical analysis

RNA was extracted with the RNeasy Mini Kit (74106; Qiagen) in combination with QIAshredder columns (79656; Qiagen) according to the manufacturer's instructions. cDNA synthesis was done with the Transcriptor Reverse Transcriptase system (03531287001; Roche) according to the manufacturer's protocols. Chromatin immunoprecipitation (ChIP) was carried out with anti-MLL^C (1:50 dilution; 05-765; Millipore/Upstate) and ChIP Kit (ab500; Abcam) according to the manufacturer's protocol. Quantitative PCR (qPCR) was conducted with a Chromo4 DNA Engine gradient cycler (PTC-200; MJ Research) and analyzed with Opticon Monitor 3 software. Statistical analysis was done with Prism 5.0d. ChIP enrichment analysis was conducted as previously described (42).

Gene expression arrays, HOXA10 ChIP studies, and bioinformatics

ChIP studies to identify HOXA10 targets were carried out with the α-HOXA10 A20 (sc-17159) and N20 antibodies (sc-17158; both from Santa Cruz Biotechnology). ChIP was carried out according to the manufacturer's protocol specified with the ChIP Kit (ab500; Abcam). Briefly, cells were fixed, lysed, and the resulting chromatin sonicated to produce fragments in the 300 to 1500 bp range. Following immunoprecipitation with the appropriate antibodies, DNA was purified according to the manufacturer's protocol. Resulting DNA was amplified with Sequenase (70775Y; US Biologicals), with some minor modifications to the manufacturer's protocol. Following quality control, the samples were used for analysis with the Affymetrix HuP1.0R platform at the TCAG microarray facility (The Hospital for Sick Children, Toronto, Ontario). Putative HOXA10 targets were identified by grouping the A20 and N20 results against a negative control obtained with no primary antibodies. Statistical significance of putative targets was determined by calculating MAT scores on T-statistics with the analysis software Partek version 6.6beta. Target validation was carried out with qPCR as described earlier.

For microarray studies, total RNA was isolated from GNS and human fetal NS cells as outlined in the above section. RNA was used for gene expression profiling at the TCAG microarray facility using the Affymetrix U133 or Gene 1.0 ST chip platforms. Statistical analysis was conducted on the Partek Genomic Suite. Some heatmaps were generated with Spotfire. Enrichment analysis was conducted with the Database for Annotation, Visualization and Integrated Discovery (DAVID) online tools (43, 44).

Short hairpin RNA constructs and transfections

5 μg of shHOXA10, the short hairpin RNA (shRNA) constructs targeting *HOXA10* (RHS4533-NM_018951; Open Biosystems), or control shRNA constructs targeting GFP (shGFP), were transfected in GNS or NS cells using the Amaxa Nucleofector Kit (VPG-1004) and a Nucleofector II electroporator (both from Amaxa Biosystems), according to the manufacturer's instructions. Approximately 1 million cells were transfected for each technical replicate. *MLL* was similarly targeted

Published OnlineFirst October 29, 2012; DOI: 10.1158/0008-5472.CAN-12-1881

with shRNA constructs (RMM3981; Open Biosystems). In this case, 2 μg of shMLL or empty pLKO.1 vector were transfected for each technical replicate.

MTT assays

MTT assays were conducted with the Cell Proliferation Kit I (11465007001; Roche) according to the manufacturer's protocol.

Results

A *HOX* signature in patient-derived GBM stem cells

Our group has developed methods for culturing precursor, or stem-like, cells from resected specimens of human high-grade gliomas in serum-free conditions, with EGF and FGF, adherently on laminin-coated plates (36, 45). Laminin has been suggested to be an important niche factor for GBM stem cells *in vitro* (46). We define the resulting primary cultures of GBM stem cells as GNS cells. GNS cells are genetically stable, they express neural precursor markers such as Nestin and SOX2 and, when transplanted in mice, they produce xenografts histologically similar to the primary tumors they originate from (ref. 36; Supplementary Table S1). For 21 of these GNS cultures, single-nucleotide polymorphism (SNP) arrays were carried out to assess their genotype (at passage number 5–7). Copy number variation data for salient GBM genes are available in Supplementary Fig. S1 and show characteristic molecular alterations seen in primary patient specimens.

In order to identify GNS-specific gene signatures, we studied gene expression profiles in GNS cells with 2 different array platforms. On a first platform (Affymetrix U133.2), we compared gene expression in 6 GNS primary cultures, 2 normal human fetal NS cell primary cultures and 6 non-neoplastic brain cortical resections (36). Gestational ages for NS cell donors are provided in Supplementary Table S2. We identified a gene expression signature consisting of *HOX* genes in GNS cells. (We hereby define the Homeobox-encoding genes in the clusters *HOXA* to *HOXD* as *HOX* genes, whereas we define the nonclustered, Homeobox-encoding genes found throughout the genome as Homeobox genes.) Interestingly, hierarchical clustering of GNS cells, NS cells, and cortical resections on the basis of expression of *HOX* genes alone segregated all samples into 2 main groups: 1 cluster populated by GNS cells and 1 including NS cells and non-neoplastic brain (Fig. 1A). This dataset suggested that *HOX* genes might play a role in the malignant behavior of patient-derived GBM stem cells and deserved further investigation. Furthermore, this clustering confirms that, at least with regard to *HOX* genes, normal NS cells seem to be an appropriate control for experiments involving GNS cells.

We used a second array platform (Affymetrix Gene 1.0 ST) to compare gene expression in a larger set of 27 GNS and 12 primary fetal NS cell cultures. This array platform offered a higher number of probes per gene and, therefore, higher sensitivity. In Fig. 1B, we show probe intensities for all *HOX* genes. This heatmap was derived by normalizing probe intensities for each GNS primary culture to the average of 12 primary NS cultures. Analysis of this larger collection of GNS cells allowed the definition of 2 groups: some GNS cells are characterized by high expression of *HOX* genes (HOX_{high} GNS cells), while others have more moderate expression of *HOX* genes (HOX_{low} GNS cells). On the basis of the results of 2 independent array platforms, we show that 19 out of 32 primary GNS cultures are HOX_{high}.

In order to investigate the notion of a *HOX* signature in a subgroup of patient-derived GNS cells further, we compared genome-wide expression data of the HOX_{high} GNS cells (13 lines) and HOX_{low} GNS cells (14 lines) as defined earlier (Fig. 1B). We identified a set of 486 differentially expressed genes between the 2 groups, setting a greater than 2-fold enrichment and ANOVA P less than 0.05 as selection criteria. Of these, 317 were significantly upregulated in HOX_{high} GNS cells compared with HOX_{low} GNS cells and were examined for enrichment of specific gene classes with DAVID. This analysis identified a significantly enriched Homeobox cluster (Fig. 2A) comprised of 18 genes (listed in Fig. 2B), including *HOX* genes found in the 4 clusters (HOXA to HOXD) and other Homeobox genes.

Bulk tumor tissue was available from 6 high-grade gliomas that gave rise to HOX_{high} GNS cells and 7 bulk tumor samples that gave rise to HOX_{low} GNS cells. These bulk tumors were used for gene expression array analysis. Unsupervised hierarchical clustering of the tumor samples was carried out on the basis of a gene set solely including *HOX* genes. Interestingly, 5 out of 6 bulk samples that gave rise to HOX_{high} GNS cells clustered in the same group (Group 2 in Fig. 2C). We identified differentially expressed genes in Group 1 and Group 2 bulk GBMs. Among the most highly upregulated genes in Group 2, we identified most of the HOX genes that also characterized HOX_{high} GNS cells (Supplementary Fig. S10). These results suggest that the *HOX* signature identified in HOX_{high} GNS cultures aligns with a gene expression profile that also characterizes the bulk patient tumor specimen. This finding suggests that a cancer stem cell signature may be identifiable in bulk GBM samples and is in line with recent findings in leukemia, consistent with an idea that at least some genes expressed in the tumorigenic stem cell programs also persist in tumor bulk (47).

Although some anterior *HOX* genes are expressed in the brain (like *HOXB1*; ref. 48), we found it interesting that most developmentally posterior *HOX* genes (for instance, *HOXA9*, *HOXA10*, *HOXC10*, and *HOXD9*) are also robustly expressed in GNS cells. Considering the established role of MLL in activation of *HOXA10* transcription in hematopoiesis and leukemic cells, we decided to further explore the existence of a Trithorax–Homeobox axis in GNS cells.

To this end, we next investigated expression of *HOXA10* by quantitative real-time PCR (qRT-PCR; Fig. 3A) in a subset of NS cells and GNS cells. In all cases, *HOXA10* was strongly expressed in GNS cells, compared with NS cells. Western blots detected HOXA10 protein in HOX_{high} GNS cells, as predicted. HOXA10 was not detectable in HOX_{low} GNS cells and in NS cells. MLL protein was detected in both NS cells and GNS cells, but its levels were higher in GNS cells (Fig. 3B).

In order to rule out the possibility that expression of MLL and HOXA10 was an artifact of our cell culture system, we

Published OnlineFirst October 29, 2012; DOI: 10.1158/0008-5472.CAN-12-1881

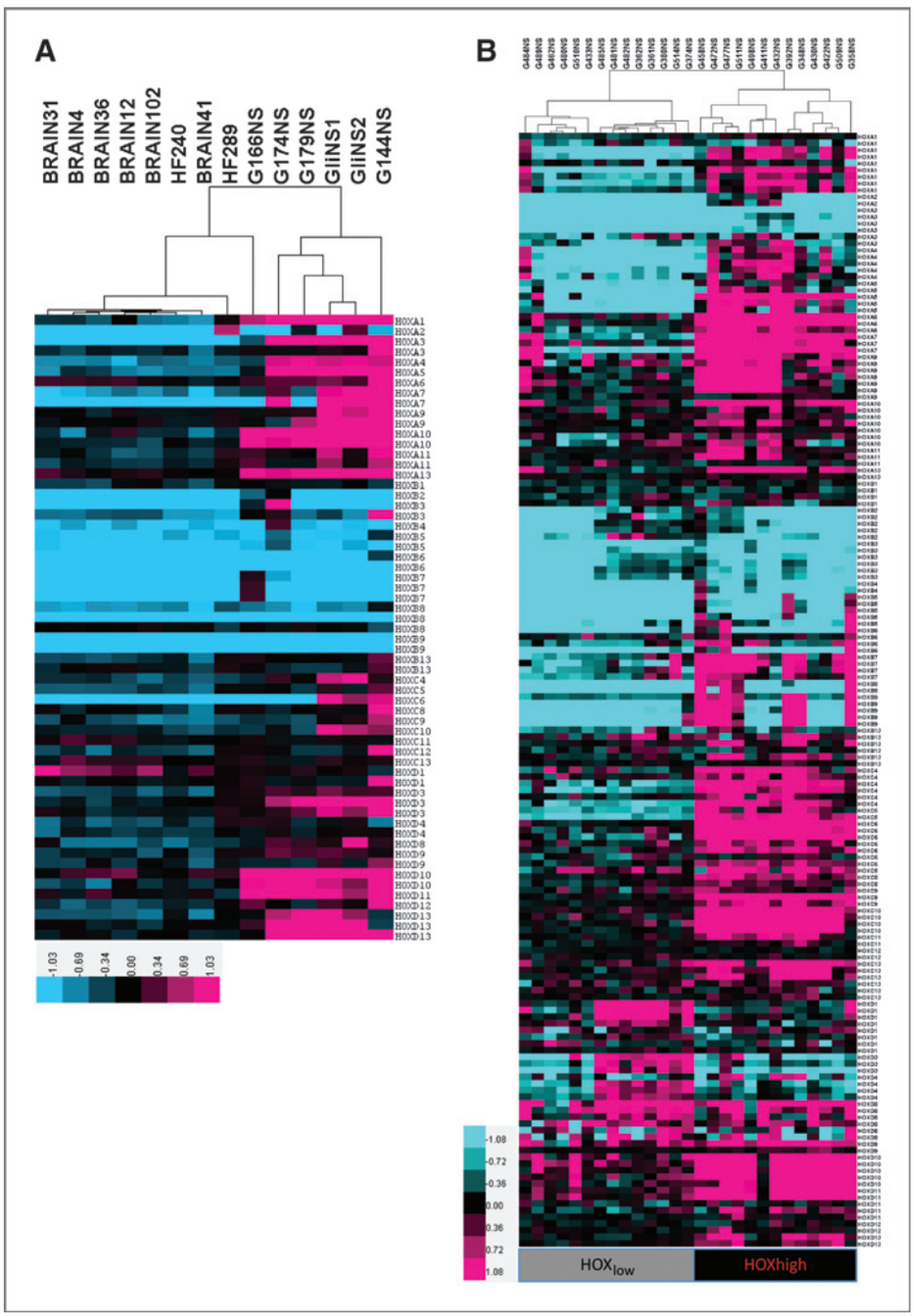

Figure 1. *HOX* signature in glioma stem cells. A, gene expression profiling of GNS cells, primary fetal NS cultures, and normal brain with the U133.2 microarray platform identified a *HOX* signature in an initial set of GNS cells. B, gene expression profiling with the Affymetrix platform Gene 1.0 ST in a further group of 27 patient-derived GNS cells identified a *HOX* signature in half of the cases. GNS cells with low *HOX* expression were defined as HOX_{low}, whereas GNS cells characterized by high *HOX* gene expression were defined as HOX_{high}. Relative intensity values were normalized to the average for 12 primary human NS cell cultures.

carried out Western blotting with cells freshly sorted for the glioma stem cell marker CD15/SSEA-1 (41) from resected GBM specimens. In all 3 cases, we observed strong MLL expression in the CD15+ fraction (Fig. 3C and D). In 1 case, we also detected enrichment of HOXA10 in the CD15+ fraction (Fig. 3D). HOXA10 was not detected in GBM481 and GBM482 (Fig. 3C). Interestingly, these primary tumors gave rise to GNS cells (G481NS and G482NS) that were classified as HOX_{low} by hierarchical clustering of microarray data (Fig. 1B). Furthermore, G481NS, the GNS cells derived from GBM481, also had HOXA10 levels that were undetectable by Western blot (Fig. 3B).

Published OnlineFirst October 29, 2012; DOI: 10.1158/0008-5472.CAN-12-1881

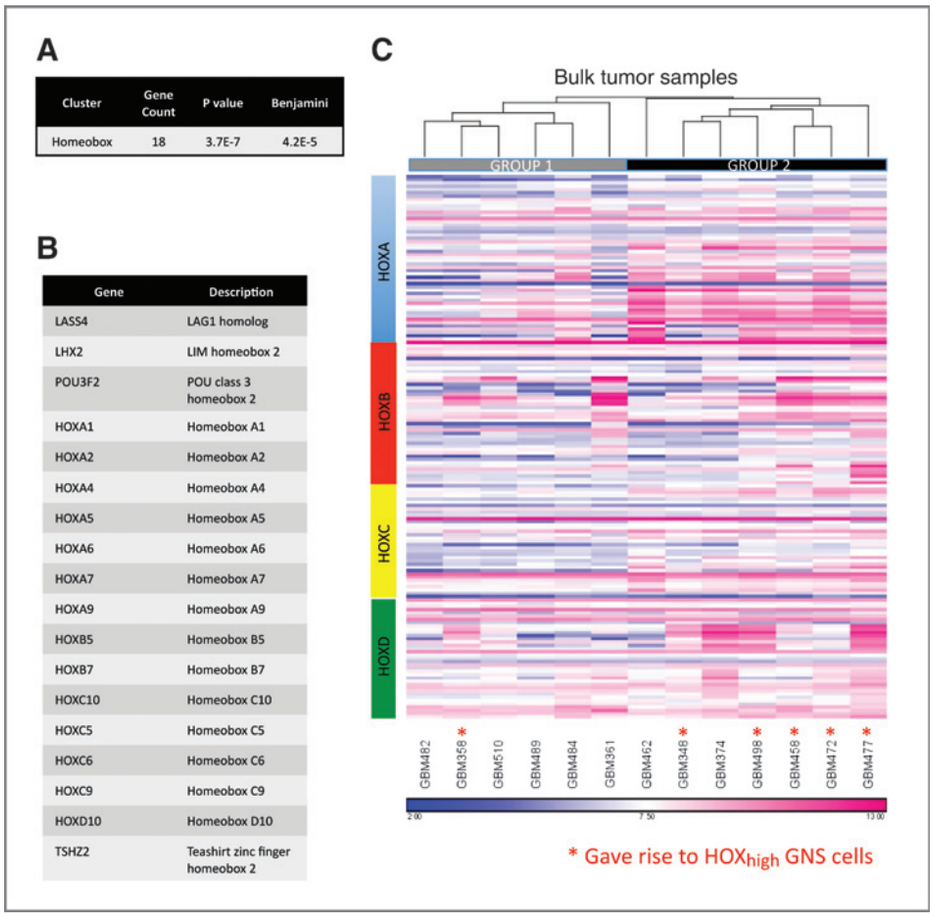

Figure 2. Identification of a Homeobox signature in a subgroup of glioma stem cells. A, comparison of HOX_{high} and HOX_{low} GNS cells identified a gene signature enriched for Homeobox transcription factors, as assessed by DAVID. B, a list of Homeobox genes that populate the Homeobox cluster identified by DAVID in A. C, unsupervised hierarchical clustering of bulk high-grade gliomas using all clustered *HOX* genes. Of the primary patient samples analyzed, 6 tumors gave rise to HOX_{high} GNS cells (red asterisks) and 5 of them clustered together in this analysis; 7 samples gave rise to HOX_{low} GNS cells. These data suggest that a *HOX* cancer stem cell signature can be detected at the expression level in primary bulk tumors.

We stained frozen sections of 1 primary GBM (GBM498) and 1 primary astrocytoma (A494) for MLL and SOX2, a marker of stemness properties. We observed strong colocalization of MLL and SOX2, suggesting expression in a precursor pool, in a subpopulation of approximately 10% of cells in both samples ($n = 356$; Fig. 3E; Supplementary Fig. S9). Single positive cells were also observed (5.6% MLL+ and 46.2% SOX2+). Similar results were obtained for 3 other paraffin-embedded primary GBM samples, where a significant fraction of SOX2+ cells were also MLL+ (Supplementary Fig. S9). Taken together, data from 8 primary brain tumors suggest that *MLL* is robustly expressed in the stem-like fraction of high-grade gliomas (marked by CD15 or SOX2) and confirms that *HOXA10* is activated in GNS cells with a HOX signature.

MLL directly regulates *HOXA10* activation in GNS cells

Our data strongly suggest that HOXA10 might play an important biological role for brain tumor stem cell function. Intrigued by the possibility of a functional MLL–HOXA10 axis in a solid tumor, we tested whether MLL physically interacts with the *HOXA10* promoter by carrying out a ChIP-PCR (ChIP followed by PCR) experiment in patient-derived GNS cells. We designed primer sets to amplify 3 different segments in the 5′-region of *HOXA10* spanning a total of approximately 2,800 bp (Fig. 4A). We carried out ChIP with an α-MLL antibody targeting the endogenous protein and found that MLL interacts with the promoter region of *HOXA10*, specifically with sequences approximately 1,380 bp upstream of the *HOXA10* translational start site (region B in Fig. 4A) in G179NS (Fig. 4B) and G411NS cells (Fig. 4C; Supplementary Fig. S8). α-H3 (an antibody against histone 3, a ubiquitous histone) was used as a positive control (Supplementary Fig. S2).

Next, in order to independently confirm a direct functional interaction between MLL and *HOXA10*, we carried out shRNA *MLL*-knockdown in G411NS cells. Forced reduction of MLL protein levels in these GNS cells resulted in a proportional decrease of HOXA10 protein levels (Fig. 4D; $P = 0.0066$ by 2-way ANOVA, based on 2 biologic replicates). Together, both the ChIP-PCR and knockdown data show a direct relationship between MLL and HOXA10 in patient-derived GNS cells.

HOXA10 confers a proliferative advantage to GNS cells

We next investigated the possibility that high levels of HOXA10 might confer a selective advantage to GNS cells by affecting their proliferation rate. We tested this possibility *in vitro* by conducting MTT assays. We transiently transfected the human GNS cells GliNS1 (Fig. 5A) and G144NS (Fig. 5B) with either a control shRNA construct targeting GFP (shGFP) or 2 shRNA constructs targeting *HOXA10* (shHOXA10-1 and shHOXA10-2; Supplementary Fig. S3). Downregulation of

Published OnlineFirst October 29, 2012; DOI: 10.1158/0008-5472.CAN-12-1881

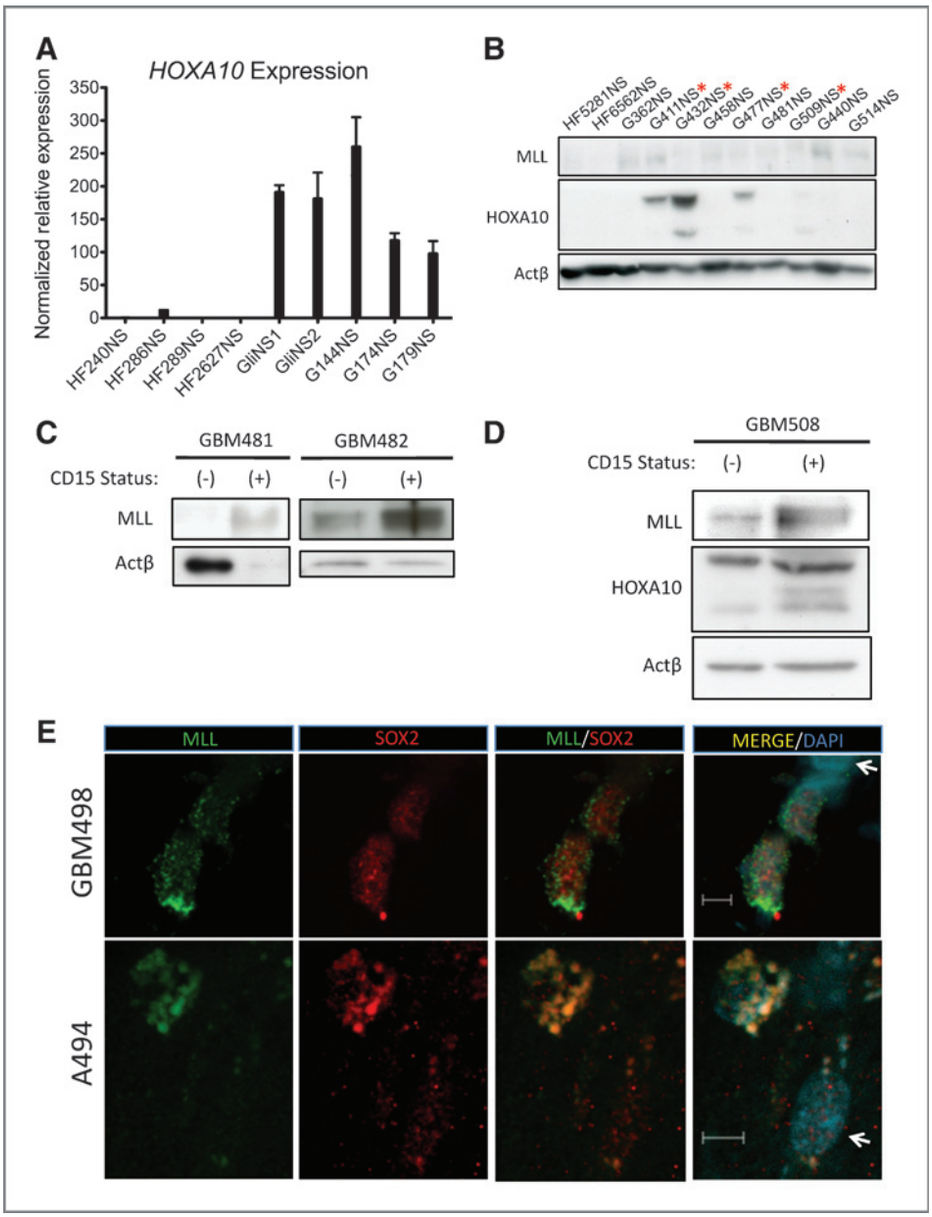

Figure 3. MLL and HOXA10 are enriched in the glioma stem cell fractions. A, qRT-PCR assays confirmed strong expression of *HOXA10* in glioblastoma neural stem (GNS) cultures compared with neural stem (NS) cell cultures. B, Western blots identified higher levels of MLL in GNS cells than in NS cells. HOXA10 was detected in GNS cells predicted to be HOX_{high} on the basis of our microarray data. HOX_{high} GNS cultures are marked by a red asterisk. C, Western blot showing enrichment of MLL protein in the CD15+ fraction of freshly resected GBMs. Unequal loading was a result of insufficient sample to allow protein quantification. D, Western blot showing enrichment of MLL and HOXA10 in the CD15+ fraction of a freshly resected GBM. E, immunohistochemistry of high-grade human glioma samples shows that MLL is expressed in SOX2+ cells in high-grade human gliomas. Arrows point to double-negative cells within the same tumors. Scale bars, 5 μm.

HOXA10 caused a robust and reproducible decrease in cell proliferation in both GliNS1 (Fig. 5A, representative of 2 independent experiments) and G144NS (Fig. 5B, representative of 2 independent experiments) cells.

As HOXA10 had an effect on GNS proliferation *in vitro*, we investigated its possible role on tumor progression in a mouse xenograft model. GliNS1 cells (Supplementary Fig. S8) carrying *HOXA10*-targeting shRNA constructs were stereotactically injected into the forebrains of NOD/SCID mice ($n = 6$). GliNS1 cells transfected with shGFP constructs ($n = 2$) or untransfected ($n = 6$) were similarly injected into mice as controls. The injected mice were monitored for the development of neurologic symptoms and the dome-head appearance conferred by brain tumors. We found that knocking down *HOXA10* in GliNS1 xenotransplants significantly increased median and maximum mouse survival compared with control (shGFP) animals (Fig. 5C, Mantel–Cox log-rank $P = 0.0039$; for full statistics see Fig. 5D). Furthermore, we attempted to knock down *HOXA10* in the 2 GNS cell cultures that have the highest level of *HOXA10* expression, namely G411NS and G432NS. We made 2 separate attempts at generating stable *HOXA10* knock-down lines from these GNS cells. In both cases, cells carrying the empty vectors were able to grow. Conversely, both G411NS and G432NS cells carrying knockdown vectors failed to grow *in vitro*. The outcomes of these experiments attest to the importance of *HOXA10* for continued GNS cell proliferation. Taken together, the results of our *in vitro* MTT assays and mouse survival in our xenotransplant model provide strong evidence that HOXA10 importantly contributes to proliferative and growth advantages of GNS cells.

Published OnlineFirst October 29, 2012; DOI: 10.1158/0008-5472.CAN-12-1881

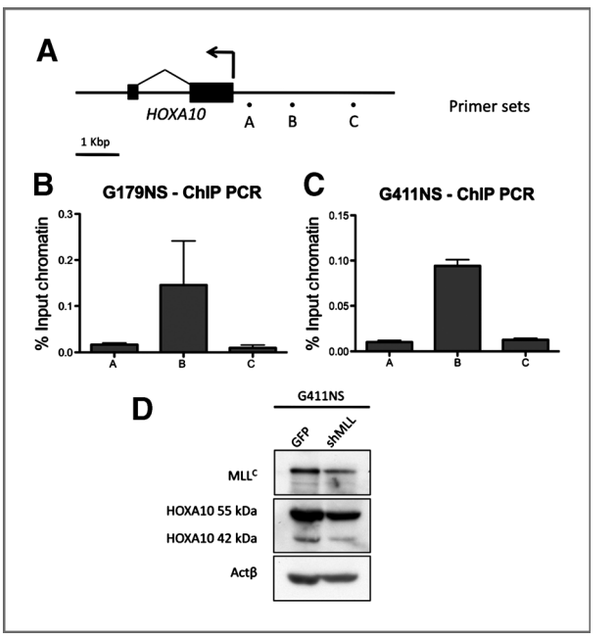

Figure 4. MLL participates in the direct regulation of *HOXA10* in GNS cells. A, schematic of the *HOXA10* locus, with A, B, and C representing the locations of primer sets designed to generate approximately 200 bp amplicons in the genomic region 5′ of *HOXA10*. B and C, ChIP-PCR using an antibody against MLL enriches for region B in G179NS and G411NS cells. D, *MLL* knockdown in G411NS cells results in decreased HOXA10 protein levels (Western blot representative of 2 separate experiments; 2-way ANOVA, $P = 0.0066$).

The MLL–HOXA10 axis maintains expression of a Homeobox gene network

Scant information on HOXA10 genome-wide target specificity exists. We therefore decided to identify putative HOXA10 targets in our GNS cells with a ChIP-chip (combining ChIP with microarray technology) strategy. Conditions were optimized to immunoprecipitate the endogenous HOXA10 protein with 2 independent antibodies (a third antibody proved less optimal for IP; see Supplementary Fig. S4 for antibody specificity) in G411NS cells. Stringent bioinformatic analysis was conducted (see Materials and Methods) and led to the discovery of 261 putative HOXA10 targets. Gene ontology analysis highlighted enrichment for the terms growth and synapse (Supplementary Fig. S5), terms consistent with a potential role of HOXA10 in malignancies of the brain. Further analysis with DAVID software found significant enrichment ($P < 0.05$) of genes in the clusters Growth factor activity, Homeobox, CHROMO domain, Cytokine, and Actin cytoskeleton organization, and an interesting, albeit not statistically significant, Chromosome organization cluster (Fig. 6A). Interestingly, some of the *HOX* genes identified in our ChIP-chip studies, namely *HOXA7* and *HOXC10*, were also part of the *HOX* signature that characterized HOX_{high} GNS cells as compared with HOX_{low} GNS cells (Fig. 2B).

As a first attempt at validating the putative HOXA10 targets, we conducted genomic qPCR on chromatin immunoprecipitated from G411NS. We validated 7 out of 7 targets using this method (Fig. 6B). Some of the identified genes with established roles in tumorigenesis and cancer stem cell biology, notably *TERT*, *FGF17*, *JAG2*, and *NODAL*, were validated as HOXA10 targets.

Evidence suggests that HOXA10 can function both as an activator and a repressor of gene expression. To gain better insights into the role of HOXA10 in GNS cell function, we looked at the expression levels of the putative targets that were enriched in the clusters identified by DAVID in our collection of GNS cells. We produced a heatmap comprising probe intensities for all genes found in the enriched DAVID clusters (Fig. 6A). Interestingly, unsupervised hierarchical clustering of GNS cells based on the expression levels of HOXA10 target genes closely recapitulated their clustering based on *HOX* gene expression (Fig. 6C). Of particular interest was the finding that HOX_{high} GNS cells had reduced levels of *IRX3* expression

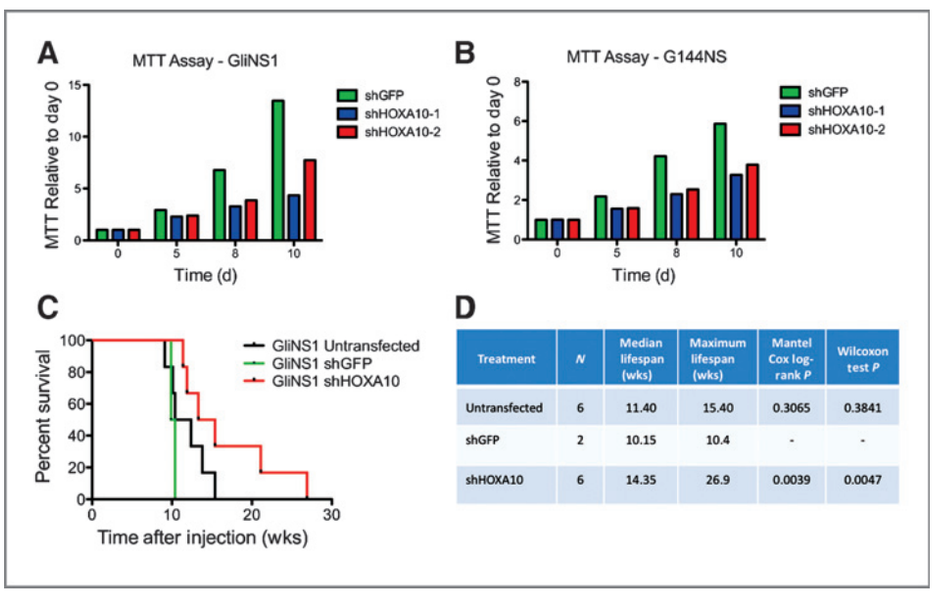

Treatment	N	Median lifespan (wks)	Maximum lifespan (wks)	Mantel Cox log-rank P	Wilcoxon test P
Untransfected	6	11.40	15.40	0.3065	0.3841
shGFP	2	10.15	10.4	-	-
shHOXA10	6	14.35	26.9	0.0039	0.0047

Figure 5. HOXA10 has a positive effect on GNS cell proliferation *in vitro* and on tumor growth in a xenograft mouse model. A and B, MTT assay illustrating that HOXA10 is required for proliferation in the GNS cells GliNS1 and G144NS. Both graphs are representative of 2 independent experiments. C, survival plot showing that knocking down *HOXA10* in GliNS1 cells before transplantation in mice increases tumor latency. Cells were injected orthotopically in NOD-SCID mice. D, complete statistical information regarding the transplantation experiments shown in C.

Published OnlineFirst October 29, 2012; DOI: 10.1158/0008-5472.CAN-12-1881

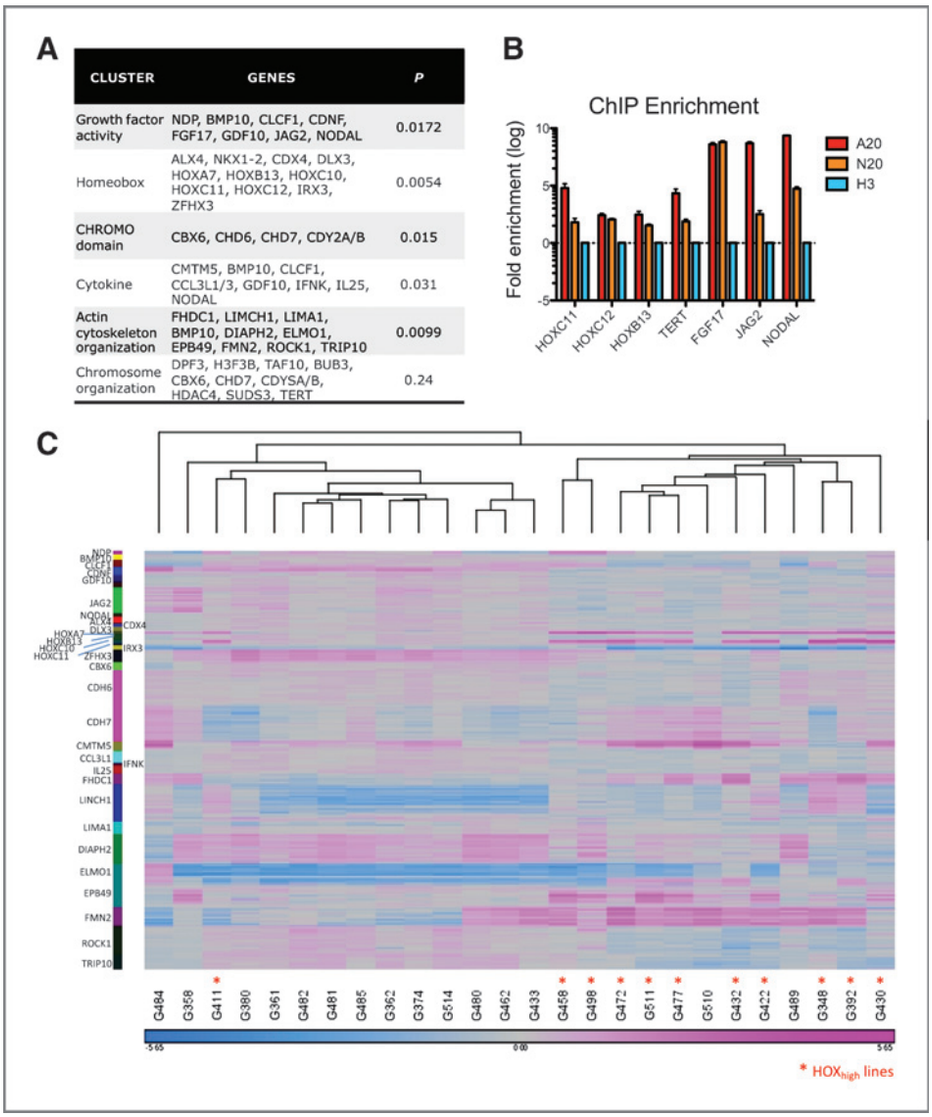

Figure 6. HOXA10 maintains a Homeobox transcriptional network. A, we conducted ChIP-chip with antibodies targeting endogenous HOXA10 to identify putative targets of this transcription factor in GNS cells. A total of 261 putative HOXA10 targets were identified. DAVID enrichment clusters are shown in this table. B, validation of HOXA10 targets by ChIP-PCR (mean ± SD). A20 and N20 are 2 independent α-HOXA10 antibodies. H3 indicates a sample obtained from immunoprecipitation with an α-Histone 3 antibody, which was used as a positive control. C, unsupervised hierarchical clustering of DAVID-enriched genes. Expression of genes shown in the 5 significantly enriched clusters in A was analyzed and unsupervised hierarchical clustering was carried out. HOX_{high} GNS cells (marked by an asterisk) tend to cluster together based on the expression of these putative HOXA10 targets.

compared with HOX_{low} GNS cells. The *IRX3* locus is known to be hypermethylated and silenced in brain tumors (49), but it appears to be further silenced in HOX_{high} cells.

In addition, we noticed that 36 of the 261 putative HOXA10 targets have an established role in leukemia, based on published evidence (Supplementary Table S3). Unsupervised hierarchical clustering was carried out on the basis of the expression profiles of these genes. As seen in the dendrogram in Supplementary Fig. S7, GNS cultures with a HOX signature tend to cluster together, suggesting that expression of these genes might truly be controlled by HOXA10.

In addition, we validated HOXA10 binding to *HOXA7*, *HOXC10*, and the chromobox-encoding *CBX6* promoters by genomic qPCR (Fig. 7A). In order to further assess the functionality of this MLL–Homeobox axis we identified, we decided to perturb the axis upstream and interrogate the downstream effects. We, therefore, knocked down *MLL* in G411NS, G432NS, and G511NS and evaluated its effects on expression of *HOXA10* and the HOXA10 targets *HOXA7*, *HOXC10*, and *CBX6*. Our results indicate that expression of *HOXA10* and its targets is dependent on *MLL* expression (Fig. 7B–D).

Discussion

In the present study, we provide evidence that GBMs are characterized by heterogeneous populations of cells with respect to their epigenetic properties. Specifically, we found enrichment of MLL in the CD15+ fraction of cells sorted from freshly resected GBM samples and in the SOX2+ fraction in high-grade glioma samples. In addition, we found robust expression of Homeobox genes in about half the GNS cells we profiled. Interestingly, the epigenetic modifier MLL was detected at the protein level in all the GNS cells we examined, and at higher levels than in normal NS cells. The different behavior of MLL in cells with high *HOXA10* expression and low *HOXA10* expression cannot be merely attributed to levels of

Published OnlineFirst October 29, 2012; DOI: 10.1158/0008-5472.CAN-12-1881

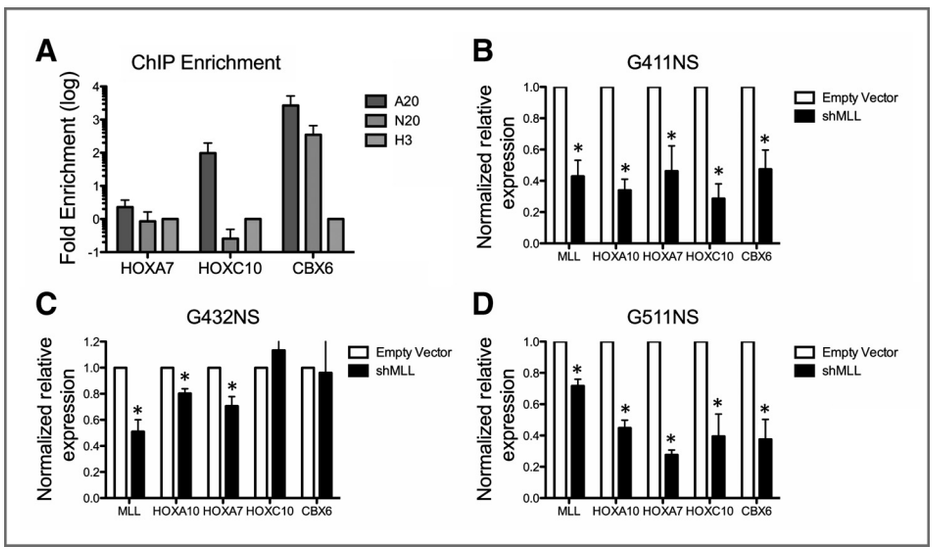

Figure 7. A functional MLL-HOXA10 axis in GBM stem cells. A, ChIP-PCR validates *HOXA7*, *HOXC10*, and *CBX6* as HOXA10 targets (mean ± SD). B–D, shRNA against *MLL* (shMLL) caused decreased expression of *HOXA10* and its downstream targets in 3 different GNS cell cultures (mean ± SD; *, $P < 0.01$). Expression levels were normalized to the housekeeping genes *GAPDH* and *Act*β. The results of these experiments show that knocking down *MLL* results in decreased expression of *HOXA10* and of its downstream targets.

this TrxG protein, as shown by our expression studies. We believe other epigenetic mechanisms regulating MLL function are at play and we are currently pursuing them actively.

We provide strong evidence in support of a functional MLL–HOXA10 axis in glioma stem-like cells. This finding is surprising because *HOXA10* was not known to be expressed in the brain or other anterior structures, suggesting that this represents aberrant activation of a developmental program in cancer cells. Frequent duplications of chromosome 7, the site of the *HOXA10* locus, are found in GBM. However, the strong expression of *HOXA10* we detected in GNS cells was from several to many orders of magnitude higher than in normal NS cells, thus suggesting that high *HOXA10* expression is a specific and biologically relevant feature linked to GBM stem cell properties and not simply due to chromosome 7 duplication. As further evidence, not all of the *HOXA* cluster genes are overexpressed in GNS cells (see, for instance, *HOXA3* and *HOXA6* in Fig. 1A). Data mining of 138 GBM bulk samples from The Cancer Genome Atlas (5, 50, 51) confirms the absence of correlation between copy number variation at the *HOXA10* locus and *HOXA10* mRNA levels (Supplementary Fig. S6). Furthermore, the increased *HOXA10* expression was not an artifact of cell culture. First, control NS cells were grown in the same conditions without upregulation of *HOXA10*. Second, we detected increased levels of HOXA10 protein in freshly sorted cells from 1 out of 3 primary GBMs.

The present report is the first to describe the mechanism by which an important epigenetic factor, MLL, functions in GBM stem cells. A recent publication identified hypoxia as a positive regulator of *MLL* in glioma cells (7). However, that report failed to identify direct MLL targets and simply focused on the coordinated expression of *MLL* and hypoxia-inducible factors under hypoxic conditions, in both GBM stem and non-stem cells. We, therefore, believe that our work provides an important conceptual advancement in the glioma stem cell field, by establishing the direct interaction between MLL and *HOXA10* and between HOXA10 and its downstream targets. We would also like to emphasize the physiologic relevance of our findings, because all the direct regulatory interactions were established by studying the endogenous proteins.

Some of the validated HOXA10 targets we identified, *TERT*, *FGF17*, *JAG2*, and *NODAL*, are of particular interest because they were previously identified as either having a role in tumorigenesis or being overexpressed in tumors with high *HOX* expression. Work in leukemia showed that the MLL-AF4 fusion protein upregulated *TERT* expression through direct regulation of *HOXA7* (52). Furthermore, a correlation between high *FGF17* and *HOXA10* expression was identified in lung cancer (53). *JAG2* was shown to be activated by a NUP98–HOXA10 fusion protein with hematopoietic stem-cell-transforming function (54). Recently, *Nodal* has been shown to be required for self-renewal and tumorigenicity of pancreatic stem cells (55). Furthermore, 1 of the most highly ranked HOXA10 targets is *CDX4*, which is a bona fide HOXA10 target in myeloid cells (56), thereby further corroborating the strength of our ChIP assay for HOXA10.

Another interesting observation was the direct regulation of other Homeobox genes by HOXA10. Some of these targets were validated 4-fold: by ChIP-array; by genomic qPCR; these genes were usually highly expressed in HOXA10-high GNS cells; and their expression decreased when the MLL–HOXA10 axis was perturbed by knocking down *MLL*. These data show that a network of Homeobox genes is activated by HOXA10, suggesting potential cooperative contributions of these transcription factors to the tumorigenic phenotype.

It is worth noting that whether we carried out hierarchical clustering of our GNS cells on the basis of expression of *HOX* genes or expression of the HOXA10 targets we identified by ChIP array, we obtained the same grouping of GNS cells. This observation suggests that HOXA10 might function as a core transcriptional node in GNS cells and reinforces the importance of the MLL–HOXA10 axis in GBM stem cell biology.

Our work and that of other researchers point to an important role of TrxG proteins in brain malignancies. A recent paper showed that 16% of medulloblastoma patients have mutations in *MLL2* or *MLL3* (30). Therefore, in addition to a contribution

Published OnlineFirst October 29, 2012; DOI: 10.1158/0008-5472.CAN-12-1881

by Polycomb proteins to tumorigenicity, our data and that of other researchers indicate that TrxG proteins and their targets also make a contribution. We propose that loss of an appropriate balance between TrxG-mediated activation and Polycomb-mediated repression of gene expression contributes to the neoplastic phenotype in GBM stem cells. The role of other TrxG proteins in GBM will be the focus of further studies.

In conclusion, the identification of a functional MLL-Homeobox network might help in the stratification of GBM patients. Fully understanding the contribution of TrxG proteins to the establishment of a glioma epigenome will be an important step to fully understand the complex biology of this disease.

Disclosure of Potential Conflicts of Interest

No potential conflicts of interest were disclosed.

Authors' Contributions

Conception and design: M. Gallo, J. Ho, I. Clarke, P. Dirks
Development of methodology: M. Gallo, J. Ho, R. Head, I. Clarke, P. Dirks
Acquisition of data (provided animals, acquired and managed patients, provided facilities, etc.): M. Gallo, J. Ho, F. Coutinho, R. Vanner, L. Lee, R. Head, E. Ling, I. Clarke, P. Dirks
Analysis and interpretation of data (e.g., statistical analysis, biostatistics, computational analysis): M. Gallo, J. Ho, I. Clarke, P. Dirks
Writing, review, and/or revision of the manuscript: M. Gallo, F. Coutinho, I. Clarke, P. Dirks
Administrative, technical, or material support (i.e., reporting or organizing data, constructing databases): L. Lee, I. Clarke
Study supervision: I. Clarke, P. Dirks

Acknowledgments

The authors thank M. Bernstein, M. Cusimano, T. Mainprize, and G. Zadeh for samples of primary brain tumor. The authors offer special thanks to Pier-Andrée Penttilä for technical expertise with FACS.

Grant Support

Financial support for this work was provided by the Canadian Institutes of Health Research (CIHR grant no. RMF-92090), the Canadian Cancer Society Research Institute (CCSRI grant no. 018047), Ontario Institute for Cancer Research (OICR grant no. STP-PRAR-HSK), Jessica's Footprint, Ontario Genomics institute, and Genome Canada.

The costs of publication of this article were defrayed in part by the payment of page charges. This article must therefore be hereby marked *advertisement* in accordance with 18 U.S.C. Section 1734 solely to indicate this fact.

Received May 15, 2012; revised September 24, 2012; accepted October 10, 2012; published OnlineFirst October 29, 2012.

References

1. Weisenberger DJ, Siegmund KD, Campan M, Young J, Long TI, Faasse MA, et al. CpG island methylator phenotype underlies sporadic microsatellite instability and is tightly associated with BRAF mutation in colorectal cancer. Nat Genet 2006;38:787–93.
2. Feinberg AP, Tycko B. The history of cancer epigenetics. Nat Rev Cancer 2004;4:143–53.
3. Noushmehr H, Weisenberger DJ, Diefes K, Phillips HS, Pujara K, Berman BP, et al. Identification of a CpG island methylator phenotype that defines a distinct subgroup of glioma. Cancer Cell 2010;17:510–22.
4. Lee J, Son MJ, Woolard K, Donin NM, Li A, Cheng CH, et al. Epigenetic-mediated dysfunction of the bone morphogenetic protein pathway inhibits differentiation of glioblastoma-initiating cells. Cancer Cell 2008;13:69–80.
5. TCGA. Comprehensive genomic characterization defines human glioblastoma genes and core pathways. Nature 2008;455:1061–8.
6. Nagarajan RP, Costello JF. Epigenetic mechanisms in glioblastoma multiforme. Semin Cancer Biol 2009;19:188–97.
7. Heddleston JM, Wu Q, Rivera M, Minhas S, Lathia JD, Sloan AE, et al. Hypoxia-induced mixed-lineage leukemia 1 regulates glioma stem cell tumorigenic potential. Cell Death Differ 2011.
8. Yi JM, Tsai HC, Glockner SC, Lin S, Ohm JE, Easwaran H, et al. Abnormal DNA methylation of CD133 in colorectal and glioblastoma tumors. Cancer Res 2008;68:8094–103.
9. Makos M, Nelkin BD, Chazin VR, Cavenee WK, Brodeur GM, Baylin SB. DNA hypermethylation is associated with 17p allelic loss in neural tumors. Cancer Res 1993;53:2715–8.
10. Sharma S, Kelly TK, Jones PA. Epigenetics in cancer. Carcinogenesis 2010;31:27–36.
11. Bruggeman SW, Hulsman D, Tanger E, Buckle T, Blom M, Zevenhoven J, et al. Bmi1 controls tumor development in an Ink4a/Arf-independent manner in a mouse model for glioma. Cancer Cell 2007;12:328–41.
12. Abdouh M, Facchino S, Chatoo W, Balasingam V, Ferreira J, Bernier G. BMI1 sustains human glioblastoma multiforme stem cell renewal. J Neurosci 2009;29:8884–96.
13. Ernst P, Mabon M, Davidson AJ, Zon LI, Korsmeyer SJ. An Mll-dependent Hox program drives hematopoietic progenitor expansion. Curr Biol 2004;14:2063–9.
14. Hess JL, Yu BD, Li B, Hanson R, Korsmeyer SJ. Defects in yolk sac hematopoiesis in Mll-null embryos. Blood 1997;90:1799–806.
15. Yagi H, Deguchi K, Aono A, Tani Y, Kishimoto T, Komori T. Growth disturbance in fetal liver hematopoiesis of Mll-mutant mice. Blood 1998;92:108–17.
16. Milne TA, Briggs SD, Brock HW, Martin ME, Gibbs D, Allis CD, et al. MLL targets SET domain methyltransferase activity to Hox gene promoters. Mol Cell 2002;10:1107–17.
17. Schuettengruber B, Martinez AM, Iovino N, Cavalli G. Trithorax group proteins: switching genes on and keeping them active. Nat Rev Mol Cell Biol 2011;12:799–814.
18. Nguyen AT, Taranova O, He J, Zhang Y. DOT1L, the H3K79 methyltransferase, is required for MLL-AF9-mediated leukemogenesis. Blood 2011;117:6912–22.
19. Bernt KM, Zhu N, Sinha AU, Vempati S, Faber J, Krivtsov AV, et al. MLL-rearranged leukemia is dependent on aberrant H3K79 methylation by DOT1L. Cancer Cell 2011;20:66–78.
20. Kawagoe H, Humphries RK, Blair A, Sutherland HJ, Hogge DE. Expression of HOX genes, HOX cofactors, and MLL in phenotypically and functionally defined subpopulations of leukemic and normal human hematopoietic cells. Leukemia 1999;13:687–98.
21. Armstrong SA, Staunton JE, Silverman LB, Pieters R, den Boer ML, Minden MD, et al. MLL translocations specify a distinct gene expression profile that distinguishes a unique leukemia. Nat Genet 2002;30:41–7.
22. Horton SJ, Grier DG, McGonigle GJ, Thompson A, Morrow M, De Silva I, et al. Continuous MLL-ENL expression is necessary to establish a "Hox Code" and maintain immortalization of hematopoietic progenitor cells. Cancer Res 2005;65:9245–52.
23. Smith LL, Yeung J, Zeisig BB, Popov N, Huijbers I, Barnes J, et al. Functional crosstalk between Bmi1 and MLL/Hoxa9 axis in establishment of normal hematopoietic and leukemic stem cells. Cell Stem Cell 2011;8:649–62.
24. Ayton PM, Cleary ML. Transformation of myeloid progenitors by MLL oncoproteins is dependent on Hoxa7 and Hoxa9. Genes Dev 2003;17:2298–307.
25. Krivtsov AV, Armstrong SA. MLL translocations, histone modifications and leukaemia stem-cell development. Nat Rev Cancer 2007;7:823–33.
26. Ferrando AA, Armstrong SA, Neuberg DS, Sallan SE, Silverman LB, Korsmeyer SJ, et al. Gene expression signatures in MLL-rearranged T-lineage and B-precursor acute leukemias: dominance of HOX dysregulation. Blood 2003;102:262–8.

Published OnlineFirst October 29, 2012; DOI: 10.1158/0008-5472.CAN-12-1881

27. Argiropoulos B, Humphries RK. Hox genes in hematopoiesis and leukemogenesis. Oncogene 2007;26:6766–76.
28. Lim DA, Huang YC, Swigut T, Mirick AL, Garcia-Verdugo JM, Wysocka J, et al. Chromatin remodelling factor Mll1 is essential for neurogenesis from postnatal neural stem cells. Nature 2009;458:529–33.
29. Lim DA, Suarez-Farinas M, Naef F, Hacker CR, Menn B, Takebayashi H, et al. *In vivo* transcriptional profile analysis reveals RNA splicing and chromatin remodeling as prominent processes for adult neurogenesis. Mol Cell Neurosci 2006;31:131–48.
30. Parsons DW, Li M, Zhang X, Jones S, Leary RJ, Lin JC, et al. The genetic landscape of the childhood cancer medulloblastoma. Science 2011;331:435–9.
31. Stupp R, Mason WP, van den Bent MJ, Weller M, Fisher B, Taphoorn MJ, et al. Radiotherapy plus concomitant and adjuvant temozolomide for glioblastoma. N Engl J Med 2005;352:987–96.
32. Costa BM, Smith JS, Chen Y, Chen J, Phillips HS, Aldape KD, et al. Reversing HOXA9 oncogene activation by PI3K inhibition: epigenetic mechanism and prognostic significance in human glioblastoma. Cancer Res 2010;70:453–62.
33. Murat A, Migliavacca E, Gorlia T, Lambiv WL, Shay T, Hamou MF, et al. Stem cell-related "self-renewal" signature and high epidermal growth factor receptor expression associated with resistance to concomitant chemoradiotherapy in glioblastoma. J Clin Oncol 2008;26:3015–24.
34. Gaspar N, Marshall L, Perryman L, Bax DA, Little SE, Viana-Pereira M, et al. MGMT-independent temozolomide resistance in pediatric glioblastoma cells associated with a PI3-kinase-mediated HOX/stem cell gene signature. Cancer Res 2010;70:9243–52.
35. Galli R, Binda E, Orfanelli U, Cipelletti B, Gritti A, De Vitis S, et al. Isolation and characterization of tumorigenic, stem-like neural precursors from human glioblastoma. Cancer Res 2004;64:7011–21.
36. Pollard SM, Yoshikawa K, Clarke ID, Danovi D, Stricker S, Russell R, et al. Glioma stem cell lines expanded in adherent culture have tumor-specific phenotypes and are suitable for chemical and genetic screens. Cell Stem Cell 2009;4:568–80.
37. Sun Y, Pollard S, Conti L, Toselli M, Biella G, Parkin G, et al. Long-term tripotent differentiation capacity of human neural stem (NS) cells in adherent culture. Mol Cell Neurosci 2008;38:245–58.
38. Reynolds BA, Weiss S. Generation of neurons and astrocytes from isolated cells of the adult mammalian central nervous system. Science 1992;255:1707–10.
39. Singh SK, Clarke ID, Terasaki M, Bonn VE, Hawkins C, Squire J, et al. Identification of a cancer stem cell in human brain tumors. Cancer Res 2003;63:5821–8.
40. Singh SK, Hawkins C, Clarke ID, Squire JA, Bayani J, Hide T, et al. Identification of human brain tumour initiating cells. Nature 2004; 432:396–401.
41. Son MJ, Woolard K, Nam DH, Lee J, Fine HA. SSEA-1 is an enrichment marker for tumor-initiating cells in human glioblastoma. Cell Stem Cell 2009;4:440–52.
42. Frank SR, Schroeder M, Fernandez P, Taubert S, Amati B. Binding of c-Myc to chromatin mediates mitogen-induced acetylation of histone H4 and gene activation. Genes Dev 2001;15:2069–82.
43. Huang da W, Sherman BT, Lempicki RA. Systematic and integrative analysis of large gene lists using DAVID bioinformatics resources. Nat Protoc 2009;4:44–57.
44. Huang da W, Sherman BT, Lempicki RA. Bioinformatics enrichment tools: paths toward the comprehensive functional analysis of large gene lists. Nucleic Acids Res 2009;37:1–13.
45. Conti L, Pollard SM, Gorba T, Reitano E, Toselli M, Biella G, et al. Niche-independent symmetrical self-renewal of a mammalian tissue stem cell. PLoS Biol 2005;3:e283.
46. Lathia JD, Gallagher J, Heddleston JM, Wang J, Eyler CE, Macswords J, et al. Integrin alpha 6 regulates glioblastoma stem cells. Cell Stem Cell 2010;6:421–32.
47. Eppert K, Takenaka K, Lechman ER, Waldron L, Nilsson B, van Galen P, et al. Stem cell gene expression programs influence clinical outcome in human leukemia. Nat Med 2011;17:1086–93.
48. Wilkinson DG, Bhatt S, Cook M, Boncinelli E, Krumlauf R. Segmental expression of Hox-2 homoeobox-containing genes in the developing mouse hindbrain. Nature 1989;341:405–9.
49. Ordway JM, Bedell JA, Citek RW, Nunberg A, Garrido A, Kendall R, et al. Comprehensive DNA methylation profiling in a human cancer genome identifies novel epigenetic targets. Carcinogenesis 2006;27: 2409–23.
50. TCAG. Comprehensive genomic characterization defines human glioblastoma genes and core pathways. Nature 2008;455: 1061–8.
51. Verhaak RG, Hoadley KA, Purdom E, Wang V, Qi Y, Wilkerson MD, et al. Integrated genomic analysis identifies clinically relevant subtypes of glioblastoma characterized by abnormalities in PDGFRA, IDH1, EGFR, and NF1. Cancer Cell 2010;17:98–110.
52. Gessner A, Thomas M, Castro PG, Buchler L, Scholz A, Brummendorf TH, et al. Leukemic fusion genes MLL/AF4 and AML1/MTG8 support leukemic self-renewal by controlling expression of the telomerase subunit TERT. Leukemia 2010;24:1751–9.
53. Calvo R, West J, Franklin W, Erickson P, Bemis L, Li E, et al. Altered HOX and WNT7A expression in human lung cancer. Proc Natl Acad Sci U S A 2000;97:12776–81.
54. Palmqvist L, Pineault N, Wasslavik C, Humphries RK. Candidate genes for expansion and transformation of hematopoietic stem cells by NUP98-HOX fusion genes. PLoS ONE 2007;2:e768.
55. Lonardo E, Hermann PC, Mueller MT, Huber S, Balic A, Miranda-Lorenzo I, et al. Nodal/activin signaling drives self-renewal and tumorigenicity of pancreatic cancer stem cells and provides a target for combined drug therapy. Cell Stem Cell 2011;9:433–46.
56. Bei L, Huang W, Wang H, Shah C, Horvath E, Eklund E. HoxA10 activates CDX4 transcription and Cdx4 activates HOXA10 transcription in myeloid cells. J Biol Chem 2011;286:19047–64.

Published OnlineFirst October 29, 2012; DOI: 10.1158/0008-5472.CAN-12-1881

Cancer Research
The Journal of Cancer Research (1916–1930) | The American Journal of Cancer (1931–1940)

AACR American Association for Cancer Research

A Tumorigenic MLL-Homeobox Network in Human Glioblastoma Stem Cells

Marco Gallo, Jenny Ho, Fiona J. Coutinho, et al.

Cancer Res 2013;73:417-427. Published OnlineFirst October 29, 2012.